

Long term response of glass–PVB double-lap joints

Luigi Biolzi^a, Emanuele Cagnacci^b, Maurizio Orlando^{b,*}, Lorenzo Piscitelli^b, Gianpaolo Rosati^c

^a Department of Architecture, Built Environment and Construction Engineering, Politecnico di Milano, Italy

^b Department of Civil and Environmental Engineering, Università degli Studi di Firenze, Italy

^c Department of Civil and Environmental Engineering, Politecnico di Milano, Italy

Received 8 January 2014
Received in revised form 10 March 2014
Accepted 24 March 2014
Available online 1 April 2014

1. Introduction

Laminated glass (LG) is a composite structure typically made of glass plies bonded by a polymeric interlayer [1] under a treatment at high pressure and temperature. As a result of this process, a strong chemical bond develops between materials, due to the union between hydroxyl groups along the polymer and silanol groups on the glass surface. It is a coupling where glass plies, made of brittle material par excellence [2], are connected using an interlayer with thermo-viscoelastic response. In laminated glass, failure of a glass element will lead to changed internal forces in the other glass elements and thus a load relocation. Due to the interlayer, the post-glass fracture phase is significantly improved because the fragments remain connected to the interlayer and consequently the possibility of injuries and the risk of catastrophic failures is reduced. In addition, the presence of interlayer enhances sound and thermal insulation capability and increases ultraviolet absorption. From a mechanical point of view, the interlayer generates the shear coupling of the glass plies, so that the response of laminated glass is intermediate between the two borderline situations of layered limit (frictionless sliding of glass plies) and monolithic limit (perfect shear bond) [3–5]. A variety of materials have been considered for the interlayer, and among which, Polyvinyl Butyral (PVB)

and Ionoplastic Polymers (IP) are the two most frequently used in practice. Commercial PVB is a random ter-polymer of vinyl butyral, vinyl alcohol and vinyl acetate with addition of plasticizer that improve mechanical properties, enhancing adhesion-strength and decreasing glass transition temperature T_g (down to about 20 °C). However, the response of the polymer is highly viscoelastic and the temperature has a dramatic influence on rates of viscoelastic response. At relatively high temperatures, interlayer materials soften with a decrease of bond stiffness and strength. In particular, dramatic changes of viscoelastic parameters are observed across glass transition temperature [6]. While the PVB is characterized by relatively poor mechanical properties, a different material – the ionoplastic polymer, presents a relatively high stiffness, strength and glass-transition temperature ($T_g = 55$ °C) when compared with PVB [7].

The deformability of PVB allows significant relative displacements between the bonded glass plies under long-term loads (e.g. self-weight) and/or high temperatures (e.g. façade or roofing applications), as already shown by the experimental evidence or through numerical analyses [8]. Experimental results have been performed on plates [9], beams [10], little specimens [11] or with Compression Shear Tests [12]. In deflected plates and beams, shear stresses and relative displacements between glass plates are not uniform. The stress distribution depends on support conditions and on loading conditions [13–19]. An almost constant shear stress distribution upon bonded area may be easily obtained in little

* Corresponding author. Tel.: +39 0554796598; fax: +39 0554796456.
E-mail address: maurizio.orlando@unifi.it (M. Orlando).

specimens loaded in pure shear or compression-shear condition [11,12]. In addition, excessive deflections of LG beams or plates may induce an uncontrolled biaxial stress field in the interlayer. From a theoretical point of view, the response of LG structural elements has been extensively investigated in recent years [3,20–24]. A practical way to evaluate the response of a LG structural element is to consider, both glass and interlayer, as *ideal* linear elastic materials assuming, for the polymer, a relaxed shear modulus as a function of temperature and time. In particular, it has been shown [24] that the stress–strain field, evaluated with a full viscoelastic analysis, can be noteworthy different from the solution of a *simple* linear elastic problem. Therefore, it is necessary to know a highly accurate representation of the material constitutive behavior of the interlayer to perform a precise design of LG structures.

In this paper, results of an extensive experimental research, which amplifies the results available in the literature in terms of load duration and hygro-thermal conditions, are presented [25–27]. In particular, tests under long-term loads at different temperature and relative humidity, were performed. Temperatures of 50 °C, 30 °C, 20 °C, –5 °C, and –20 °C, a range that covers in practice all the operating temperatures of laminated glass in building works, were selected with the aim of investigating the behavior of the interlayer below and above the transition phase. Finally, specimens with different bonded areas and form factors of the bonded area were also tested. Experimental results were employed for material characterization applying a generalized Maxwell model to model the viscoelastic behavior (using Prony series) that provides a range of relaxation times, and a time shift function obtained from the Williams, Landel and Ferry equation.

2. Experimental procedure

2.1. Materials

Tensile tests were performed on PVB specimens shaped as in Fig. 1a. The PVB interlayer used in the laminated-glass units was 1.52 mm thick. The mechanical properties, being an elastomeric material, are considerably affected by loading rate, strain level, and temperature of the specimen [28–30]. In addition, the experimental response shows that this PVB material is highly viscoelastic. Fig. 2 presents a typical stress–strain curve in a tensile test conducted at a temperature of 20 °C imposing a displacement rate at the actuator of 10 mm/min: the stress increases with the strain in an exponent-like shape. A picture of the PVB specimen close to the final failure is also included (Fig. 1b). The tangent Young's modulus E of the PVB varied from 2.15 N/mm² initially to 14.9 N/mm² for a value of strain of 2, and remains constant for values greater than 2, up to final specimen failure. Because the Poisson's ratio is about 0.5, the shear modu-



Fig. 1. PVB specimen under uniaxial tensile test.

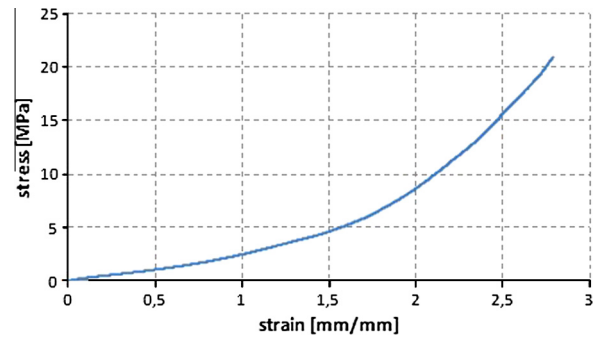


Fig. 2. Uniaxial tensile stress response of PVB specimen.

lus results $G = E/3$. The length of failed specimens were equal to those of the untested specimens in spite of failure strain was almost 300% of the original specimen length. Tests with an increased strain rate (twice faster), showed that the failure stresses remained nearly the same while the failure strain had a tendency to decrease (about 15%). As a comparison, Fig. 3 shows the uniaxial tensile stress response of a IP specimen. The constitutive behavior is significantly different from PVB; it displays elastic-plastic behavior with a noteworthy initial stiffness of about 480 N/mm², at least compared to the values measured for the PVB (the values differ by more than two orders of magnitude). In this case, the length of failed specimens were significantly different to those of the untested specimens. Note that the strengths of the two materials were not very different, but it should be observed that in the laminated glass plates or beams, only the first part of the stress–strain curve is significant. Tensile tests with a displacement rate speed at the actuator ranging from 1 mm/min to 100 mm/min did not show notable influence on the mechanical response. From a mechanical point of view, this polymer maintains significant advantages over PVB for a large range of temperature (room temperature up to 80 °C). Therefore, the IP interlayer is considerably stiffer than the PVB interlayer and hence less sensitive to viscoelastic phenomena [10].

2.2. Test setup

Tests were performed on specimens with different form factors. All specimens were assembled using 3 × 10 mm² thick glass plates bonded together using 1.52 mm PVB interlayers (Fig. 4). Eight sets of specimens were tested; each set was identified with a different code, as listed in Table 1. The test setup is shown in Fig. 5. Tests were arranged for six different climatic conditions, varying temperature, relative humidity and testing time (Table 2). The bonded PVB area is given by: $A_{tot} = 2 \cdot b \cdot d$, where b is width

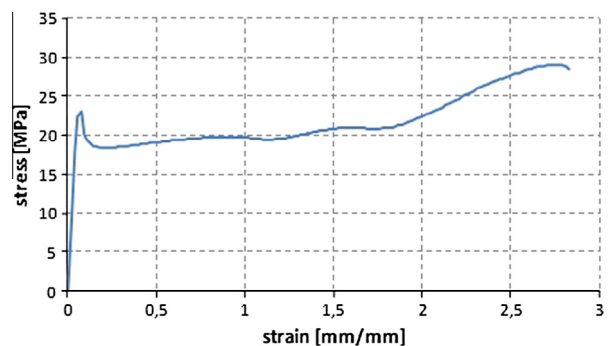


Fig. 3. Uniaxial tensile stress response of SGP specimen.

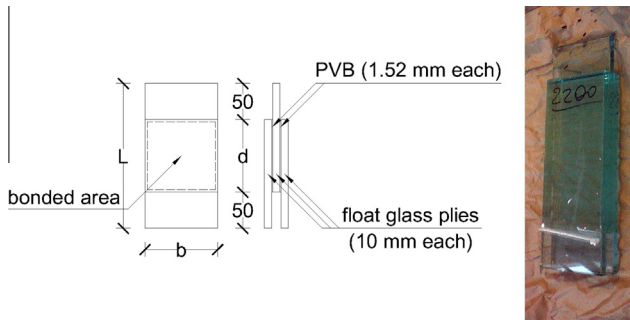


Fig. 4. Dimensions and view of a specimen.

and d is the height of the specimen over which the three plies overlap. The loading conditions were selected to reproduce an average shear stress between 0.33 N/mm^2 and 0.65 N/mm^2 . Due to the very poor mechanical properties of the interlayer as a comparison of the glass plies, the shear stresses are almost uniform in the interlayer. This is confirmed by three dimensional finite element analyses using the code ABAQUS and, according to ASTM D3983 (Standard Test Method for Measuring Strength and Shear Modulus of Nonrigid Adhesives by the Thick-Adherend

Tensile-Lap Specimen), evaluating the Shear Stress Uniformity Parameters. In any case, the viscoelasticity of the interlayer is another factor which would instigate a reduction of the stress gradients [24]. The load was applied by means of a dynamometric ring manually adjusted by a screw. At temperatures equal or higher than 20°C , shear stresses in PVB relaxed very quickly and the load had to be adjusted frequently (load was adjusted on a daily basis at least for the first week). However, frequent load regulations were not suitable because they would have required too many openings of the climatic chamber, which would have changed the test climatic conditions. Therefore, experimental results at 20°C , 30°C and 50°C showed a series of decreasing load steps at regular time intervals; no load adjustments were required for tests at -5°C and -20°C . During tests, the applied load and relative displacements between the central glass sheet and the outer glass sheets were automatically recorded. Three different climatic chambers were used for tests at $30/50^\circ\text{C}$, at 20°C and at $-5/-20^\circ\text{C}$. For 20°C tests specimens were located in a climatic room, so that it was allowed to adjust the load without interfering with the test conditions. For the other tests smaller chambers (Fig. 6) were used, which required to be left open during the load adjustments. Only virgin specimens were tested; that is no specimen was tested two or more times.

Table 1
Code and dimensions of specimen series.

Code of specimen series	b (mm)	d (mm)	l (mm)	Total bonded area (mm^2)
100 × 100	100	100	200	20,000
100 × 125	100	125	225	25,000
100 × 150	100	150	250	30,000
100 × 200	100	200	300	40,000
200 × 100	200	100	200	40,000
100 × 250	100	250	350	50,000
200 × 150	200	150	250	60,000
125 × 250	125	250	350	62,500

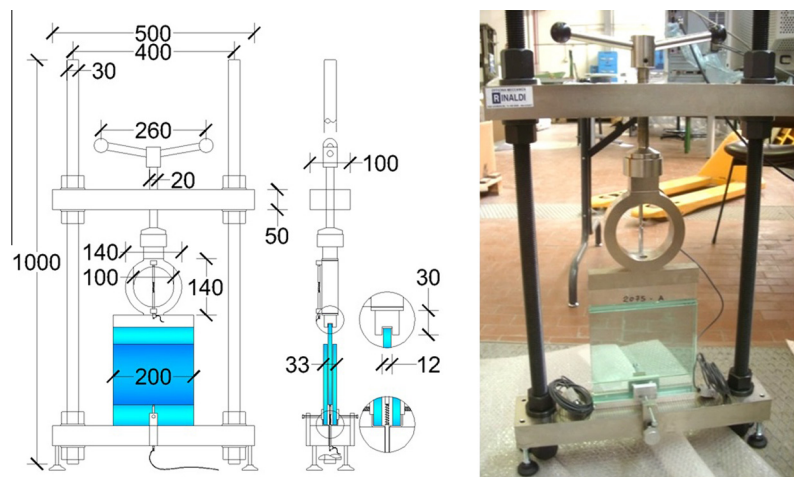


Fig. 5. Specimen installed in the steel frame.

Table 2
Climatic conditions, duration time and number of tested specimens for each series.

Temperature and relative humidity	Load time (days)	Unload time (days)	Number of tested samples	Specimen codes
50°C , 70% R.H.	13	None	5	100 × 100, 100 × 150, 100 × 125, 200 × 100, 200 × 150
30°C , 70% R.H.	30	7 (1 sample)	4	100 × 125, 100 × 150, 200 × 100, 200 × 150
20°C , 50% R.H.	37	32 (3 samples)	3	200 × 150, 200 × 100, 100 × 100
20°C , 90% R.H.	40	26 (3 samples)	3	100 × 200, 100 × 250, 125 × 250
-5°C , 50% R.H.	23	None	3	100 × 200, 100 × 250, 125 × 250
-20°C , 50% R.H.	6	None	1	100 × 250

3. Experimental results

Experimental results are collected according to decreasing temperature. For each climatic condition at least three specimens were tested, except for $-20\text{ }^{\circ}\text{C}$ where only one specimen was considered.

3.1. Tests at $50\text{ }^{\circ}\text{C}$ and 70% R.H

The diagram in Fig. 7 shows the load and displacement variations for a test at $50\text{ }^{\circ}\text{C}$ and 70% R.H. as a function of time (specimen 100×125). Tests were originally designed to be conducted for longer durations, applying a constant load over time and recording displacements. The specimens were loaded to produce an average shear stress of 0.5 N/mm^2 in the PVB interlayers. The extreme deformability showed that the selected value of the shear stress was too high; consequently, new loads were imposed to induce shear stresses in the interlayers of 0.25 N/mm^2 and 0.125 N/mm^2 , respectively. Even for those smaller stresses, the joints failed and the tests were completed considering a constant displacement over the time.

3.2. Tests at $30\text{ }^{\circ}\text{C}$ and 70% R.H

The tests were performed with a continuous adjustment of the loading rate to compensate the creep of the interlayer. One of the specimens (100×125 , Fig. 8) was also submitted to a brief unload test of 1 week. Tests were meant to be performed for stress of 0.33 N/mm^2 but due to the varying load level over time, the actual mean stress for each specimen was in the range $0.30\text{--}0.32\text{ N/mm}^2$. Similarly to tests conducted at $50\text{ }^{\circ}\text{C}$, the results showed that even at $30\text{ }^{\circ}\text{C}$ the main displacements occur just after the load adjustments; on the other side, load history showed that for this temperature PVB is much more effective in transferring shear stresses.

3.3. Tests at $20\text{ }^{\circ}\text{C}$, 50% R.H. and 90% R.H

Tests at $20\text{ }^{\circ}\text{C}$ were conducted both at 50% R.H. and 90% R.H. The results showed that the humidity level did not significantly affect the response of the interlayer at least for the applied loads and over the considered period of time. Fig. 9 shows the observed behavior for a test performed at $20\text{ }^{\circ}\text{C}$ and 50% R.H. (specimen 200×150), while Fig. 10 shows the results a test at $20\text{ }^{\circ}\text{C}$ and 90% R.H. (specimen 100×150). The load for each specimen was calibrated to induce a shear stress of 0.50 N/mm^2 , but once again because of the load relaxation over time, shear stress resulted to have average value of 0.49 N/mm^2 .



Fig. 6. View of a set of specimens inside the climatic chamber.

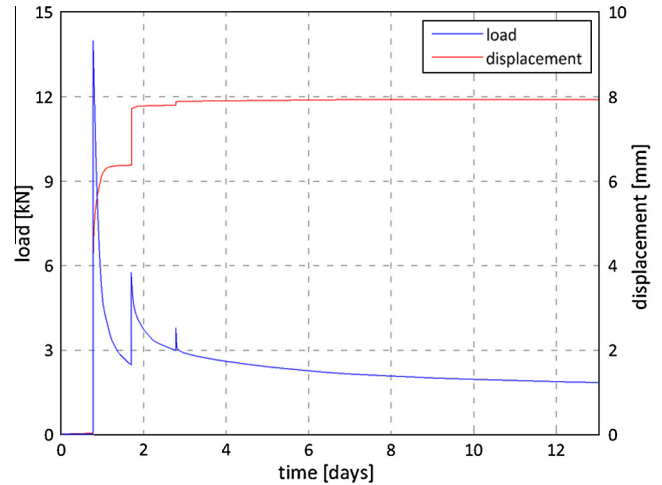


Fig. 7. Specimen 100×125 ($50\text{ }^{\circ}\text{C}/70\% \text{ R.H.}$).

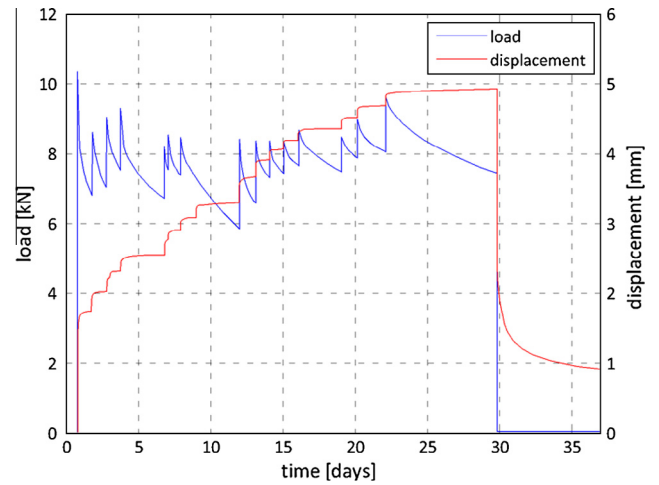


Fig. 8. Specimen 100×125 ($30\text{ }^{\circ}\text{C}/70\% \text{ R.H.}$).

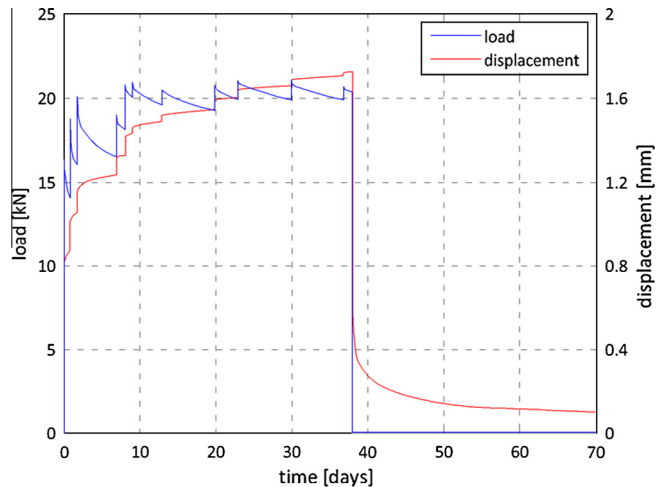


Fig. 9. Specimen 200×150 ($20\text{ }^{\circ}\text{C}/50\% \text{ R.H.}$).

3.4. Tests at $-5\text{ }^{\circ}\text{C}$ and $-20\text{ }^{\circ}\text{C}$

Below zero tests were performed on a total of five specimens, three of which tested at $-5\text{ }^{\circ}\text{C}$ (e.g. Fig. 11 for specimen 100×200) and one at $-20\text{ }^{\circ}\text{C}$ (e.g. Fig. 12 for specimen

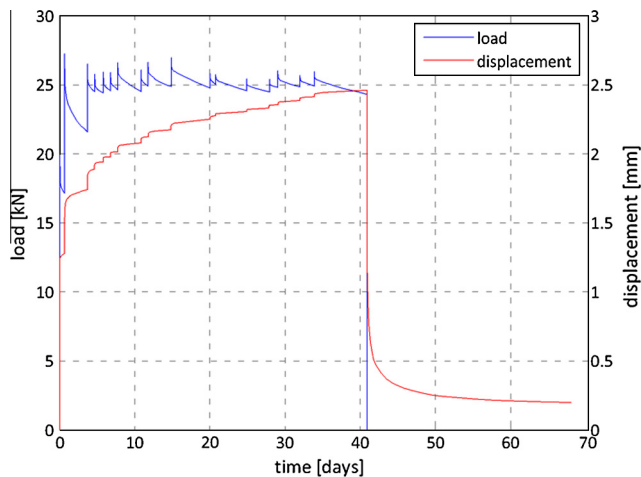


Fig. 10. Specimen 100×250 ($20\text{ }^{\circ}\text{C}/90\% \text{ R.H.}$).

100×250). The results showed how the behavior of the PVB interlayer below the transition temperature is different from the one observed at the other temperature range. The creep of the interlayer induced a more linear behavior for the displacements as a function of time, furthermore no load adjustments were required to perform tests under constant load conditions. The oscillatory aspect of the load curve is due to the small variations of temperature in the climatic chamber (approximately in-between $-7\text{ }^{\circ}\text{C}$ and $-4\text{ }^{\circ}\text{C}$). The test 100×250 at $-20\text{ }^{\circ}\text{C}$ showed how the interlayer had a very stiff response and actually made the creep phase of the PVB irrelevant.

4. Experimental evidence

As expected, creep is evident at all considered temperatures. The results showed that PVB creep effects continue to grow even for many days after the load application. In particular, at higher and intermediate temperatures displacements increase without approaching a constant value. On the other hand, at the lowest temperatures ($-5\text{ }^{\circ}\text{C}$ and $-20\text{ }^{\circ}\text{C}$) PVB behaves similarly to an elastic material, presenting no significant variation the six days in which the only specimen at $-20\text{ }^{\circ}\text{C}$ (100×250) was tested. After load removal, PVB does not return to the initial configuration, even after many days, this is probably due to a permanent plastic deformation induced in the interlayer. Concerning the humidity level, it

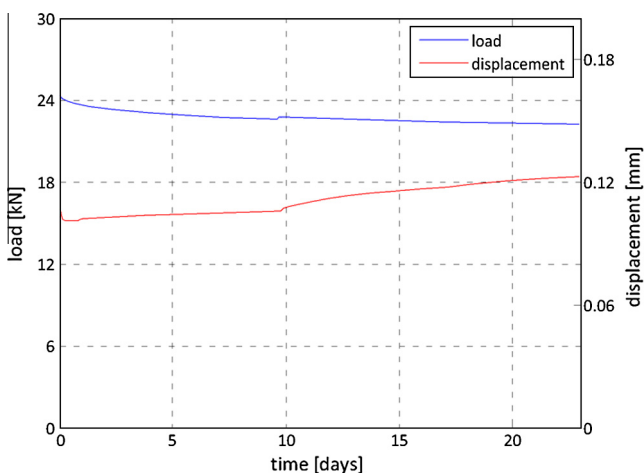


Fig. 11. Specimen 100×200 ($-5\text{ }^{\circ}\text{C}/50\% \text{ R.H.}$).

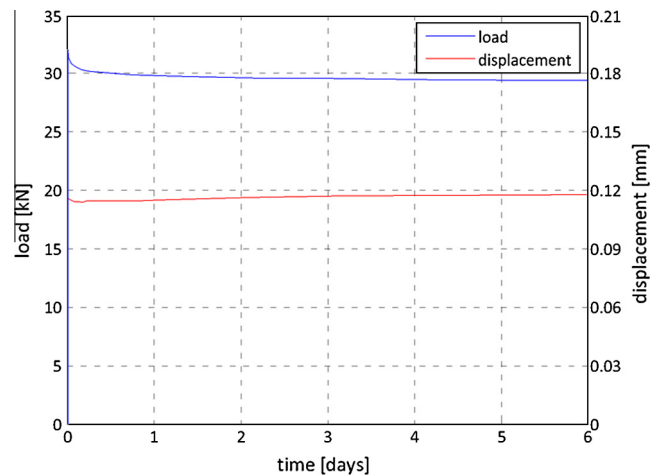


Fig. 12. Specimen 100×250 ($-20\text{ }^{\circ}\text{C}/50\% \text{ R.H.}$).

appears that the variation of the relative humidity has no significant influence on the shear modulus for loads of the duration of up to 30 days. Comparing the effective shear modulus in Table 3, the main difference concerns the results for one minute duration loads, but the test setup was not designed to investigate specifically those load conditions.

Results of tests are presented introducing the shear modulus $G(t) = \tau(t)/\gamma(t)$, where $\tau(t)$ is the mean shear stress at PVB-glass interface and $\gamma(t)$ is the shear strain. Diagrams in Figs. 13–17 show the variation of $G(t)$ over time for each considered test condition. The mean values for each climatic condition were calculated with a local linear interpolation at selected points, corresponding to intervals varying from 10 h to 1 day depending on the test conditions. Some specimens, such as 100×150 , tested at $50\text{ }^{\circ}\text{C}/70\% \text{ R.H.}$ (Fig. 13), and the 200×150 tested at $30\text{ }^{\circ}\text{C}/70\% \text{ R.H.}$ (Fig. 14), showed a substantially different behavior compared to results of specimens tested at the same climatic conditions, this seems to be a consequence of the different form factor. More tests are required to confirm these results and/or provide enough data to perform a statistical analysis of the phenomena.

Fig. 18 presents a summary of the results concerning the mean shear modulus $G(t)$ for all the climatic conditions in a semi-logarithmic graph. The figure shows how a linear interpolation in a semi-logarithmic graph is an acceptable approximation at least for tests concerning below-zero, $20\text{ }^{\circ}\text{C}$ and $30\text{ }^{\circ}\text{C}$ climatic conditions.

The mean value of $G(t)$ for each considered condition as a function of time is presented in Table 3. The shear modulus indicated for load application of one minute has to be taken solely as an estimate and an indication of the order of magnitude, because the test setup was not specifically designed to investigate the effects of short duration loads. These results confirm data obtained if one uses the time-temperature superposition principle [28–31].

4.1. Viscoelastic constitutive response

To predict the stress-strain response of polymers is a difficult problem because their complex thermo-mechanical behavior. A polymer does not relax with a single relaxation time and cannot be modeled by the simple spring-dashpot models. The simpler and shorter molecular segments relax much more quickly than the long ones. As a consequence, a distribution of relaxation times with a relaxation spread over a much longer time have to be considered. In this context, a general model for linear viscoelasticity is the Wiechert model (also known as generalized Maxwell model or

Table 3
Registered values of G in time for different climatic conditions.

	G (N/mm ²) vs. climatic conditions and load duration						
	1 min	1 day	5 days	10 days	15 days	30 days	
50 °C 70% R.H.	0.30	0.03	0.02	0.01	–	–	
30 °C 70% R.H.	0.70	0.31	0.23	0.19	0.18	0.12	
20 °C 50% R.H.	1.60	0.46	0.41	0.38	0.36	0.33	
20 °C 90% R.H.	1.30	0.47	0.40	0.37	0.36	0.33	
–5/–20 °C 70% R.H.	8.50	7.95	7.62	7.28	6.74	–	

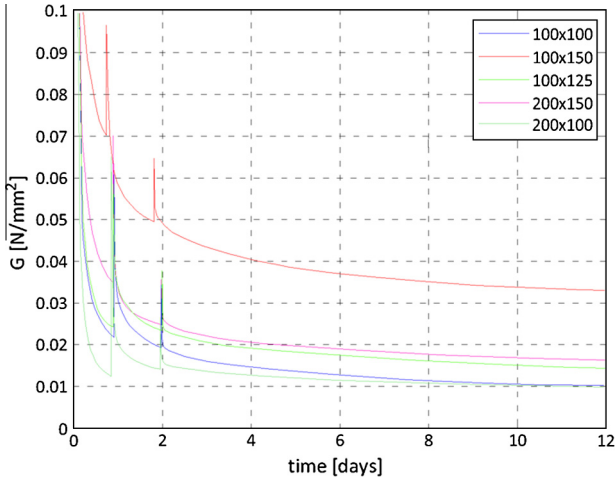


Fig. 13. Shear modulus at 50 °C and 70% R.H.

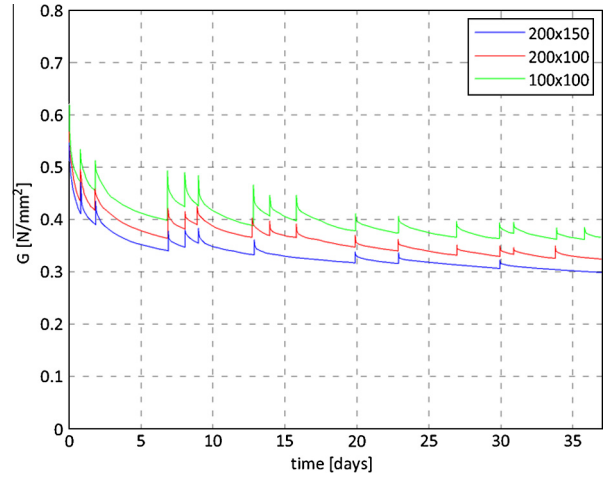


Fig. 15. Shear modulus at 20 °C and 50% R.H.

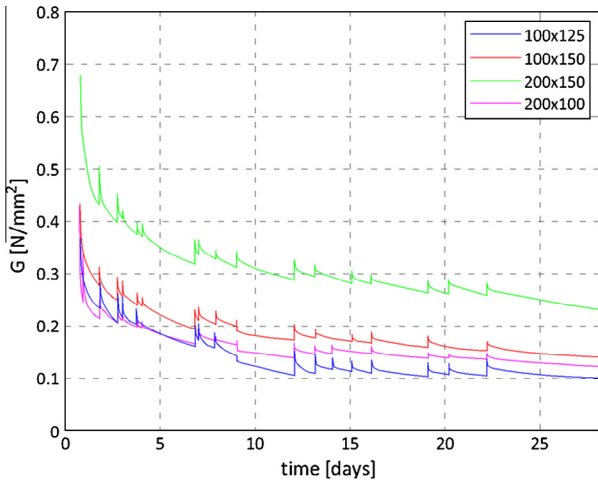


Fig. 14. Shear modulus at 30 °C and 70% R.H.

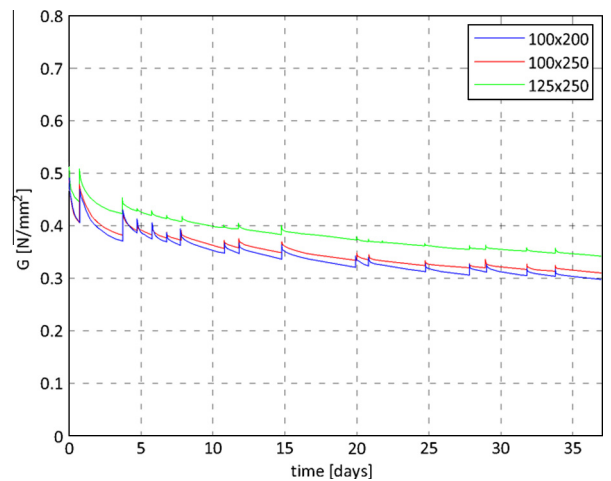


Fig. 16. Shear modulus at 50 °C and 90% R.H.

a Maxwell-Weichert model) [31], schematically exemplified in Fig. 19, which combines in parallel a series of Maxwell spring-dashpot units and a Hookean spring. In this model the relaxation does not occur at a single time-scale, but at a number of different time scales, each one associated with a Maxwell unit. When exposed to a fixed constant shear-stress, the shear modulus of the viscoelastic material decays with time can be effectively modeled by what is usually referred to as Prony series [32,33], defined as:

$$G(t) = G_0 + \sum_{i=1}^n G_i \cdot e^{-\frac{t}{\tau_i}}$$

where $G(t)$ is the time-dependent shear modulus, G_0 is the long term shear modulus, and G_i and τ_i are the relaxation terms and

the time constants, respectively. Three to four decaying terms ($n = 3$ or 4) are commonly required to completely define the time-dependent shear modulus $G(t)$. Consequently, seven or nine parameters have to be determined to accurately determine $G(t)$ at a given temperature, respectively. $G(t)$ was identified via a four term Prony series and the coefficients determined from the curve fitting (see Fig. 20) are presented in Table 4.

Combining the various Prony series obtained at the temperature levels from 20 °C to 50 °C, a single Prony series master curve to describe the viscoelastic behavior can be identified for the shear modulus of the material (Fig. 21). The coefficients determined from the master curve are presented in Table 5. The Prony series curve at 20 °C was not shifted and was used as the reference curve.

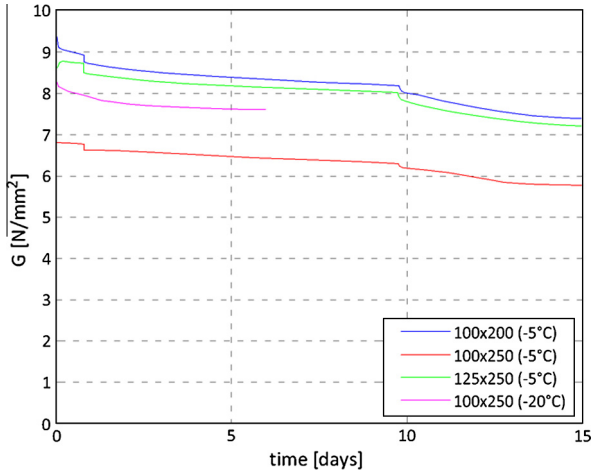


Fig. 17. Shear modulus at -5°C and -20°C , 70% R.H.

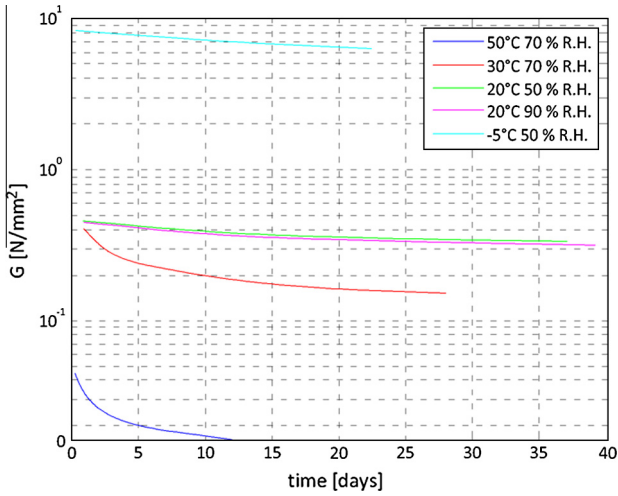


Fig. 18. Average shear modulus for different climatic conditions.

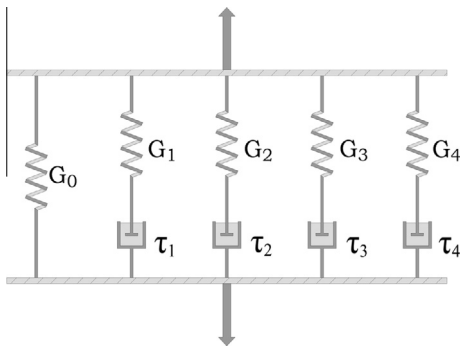


Fig. 19. Wiechert model.

One of the most common functions relating the shift factor a_T and temperature T has been proposed by Williams, Landel and Ferry [31] as follows

$$\log a_T = \frac{-C_1(T - T_{ref})}{C_2 + (T - T_{ref})}$$

where C_1 and C_2 are material constants and T_{ref} is the reference temperature. This form is referred to as the WLF equation. This equation

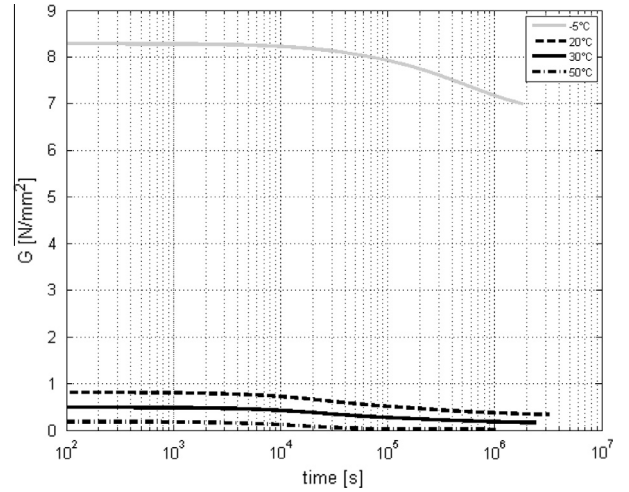


Fig. 20. Time dependent shear modulus (Prony series) at all investigated temperatures.

Table 4

Relaxation terms and time constants of Prony series for each considered temperature.

Temperature	i	G_i (MPa)	τ_i (days)
-5°C	0	6.297	–
	1	0.060	0.340
	2	0.396	1.080
	3	0.863	10.319
	4	0.669	18.815
20°C	0	0.307	–
	1	0.289	1.176
	2	0.024	8.092
	3	0.052	18.417
	4	0.023	37.005
30°C	0	0.143	–
	1	0.118	0.480
	2	0.074	3.235
	3	0.063	12.728
	4	0.021	25.932
50°C	0	0.016	–
	1	0.142	0.192
	2	0.015	1.230
	3	0.008	4.385
	4	0.002	10.770

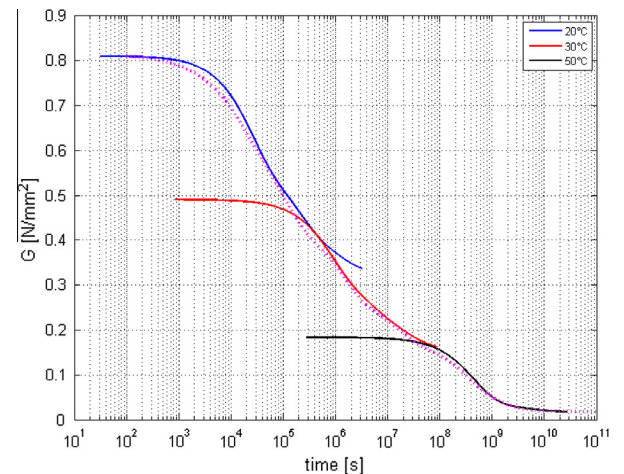


Fig. 21. Shifted Prony series curves for 20°C , 30°C , 50°C and master curve (dotted line).

Table 5
Relaxation terms and time constants of master curve Prony series.

i	G_i (MPa)	τ_i (s)
0	0.018	-
1	0.017	$1.047 \cdot 10^3$
2	0.138	$1.202 \cdot 10^4$
3	0.216	$8.832 \cdot 10^4$
4	0.172	$1.299 \cdot 10^6$
5	0.097	$1.537 \cdot 10^7$
6	0.098	$3.063 \cdot 10^8$
7	0.053	$1.319 \cdot 10^9$
8	0.004	$1.496 \cdot 10^{10}$

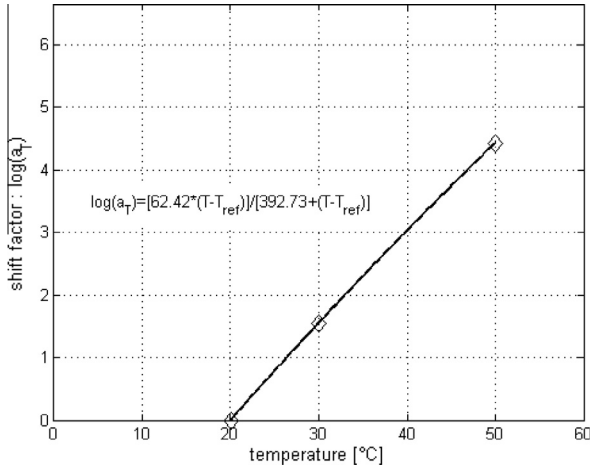


Fig. 22. Shift factors.

has been used to describe the temperature effect on the relaxation behavior of many polymers with satisfactory results [31]. Therefore, the WLF shift factor interpolation for temperatures between 20 °C and 50 °C gives:

$$\log a_T = \frac{62.42 \cdot (T - T_{ref})}{392.72 + (T - T_{ref})}$$

The corresponding shift factors were then obtained and are plotted in Fig. 22.

The shift function and the master Prony series terms must collected and implemented into a commercial finite element package during non-isothermal numerical simulations.

5. Conclusions

In this paper, the response of laminated PVB-glass under long duration loading at different temperature and relative humidity, was investigated. Experimental results confirm the high sensitivity of PVB to both temperature and load duration. For long-term loads and most engineering applications, the effective shear modulus tends to vanish for temperatures higher than 30 °C. On the other hand, at temperatures below 0 °C, the shear modulus G has been proven to be greater than 0.5 N/mm² even under long-term loads. For intermediate temperatures (20–30 °C), a null shear modulus should be considered depending on the applications and design load history. Tests at 50 °C have been performed for a reduced time interval, due to the extremely low value of the PVB shear modulus at high temperatures combined with the high stiffness of the test setup.

Regarding the level of relative humidity and the aspect ratio of specimens, they did not appear to have a significant influence on

the mechanical properties of the interlayer. However, the behavior of some specimens tested at 30 °C and 50 °C suggests that an extension of the experimental campaign is required, in order to collect enough data for a statistical analysis.

The shear moduli in the form of a four terms Prony series were obtained. Time temperature superposition has been conducted to get the master curve using an eight terms Prony series. The WLF equation was selected as function connecting temperature and shift function.

Acknowledgements

The authors gratefully acknowledge funding from the Italian Ministry of Education, University and Research (MIUR), Eng. Veronica F. Fumagalli for help in data recording and analysis, and Prof. Paolo Spinelli for critical discussions and suggestions. In addition, the authors gratefully acknowledge the reviewers for their beneficial comments and suggestions to improve the paper.

References

- [1] CEN EN ISO 12543-1. Glass in building. Laminated glass and laminated safety glass. Definitions and description of component parts; 2011.
- [2] Badalassi M, Biolzi L, Royer-Carfagni G, Salvatore W. Calibration of partial safety factors for the structural design of glass. *Constr Build Mater* 2014;55:114–27.
- [3] Galuppi L, Royer-Carfagni G. The effective thickness of laminated glass plates. *J Mech Mater Struct* 2012;7:375–400.
- [4] Gräf H, Albrecht G, Sackmann V, Schuler C, Bucak Ö. Structural behaviour of point-supported and clamped laminated glass. *Struct Eng Int* 2004;2:129–33.
- [5] Galuppi L, Royer-Carfagni G. The design of laminated glass under time dependent loading. *Int J Mech Sci* 2013;68:67–75.
- [6] Bennison SJ, Jagota A, Smith CA. Fracture of glass/polyvinyl butyral laminates in biaxial flexure. *J Am Ceram Soc* 1999;82:1761–70.
- [7] Bennison SJ, Davies PS, Van Duser A, Jagota A. Structural performance of laminated safety glass made with “stiff” interlayers. In: *Proceedings of glass performance days, Tampere (Finland); 2001.*
- [8] Aşık MZ, Tezcan S. A mathematical model for the behavior of laminated glass beams. *Comput Struct* 2005;83:1742–53.
- [9] Aşık MZ, Tezcan S. Laminated glass beams: strength factor and temperature effect. *Comput Struct* 2006;84:364–73.
- [10] Biolzi L, Cattaneo S, Rosati G. Progressive damage and fracture of laminated glass beams. *Constr Build Mater* 2010;24(4):577–84.
- [11] Cagnacci E, Foconi R, Orlando M, Spinelli P. Numerical simulation and experimental analysis of PVB Interlayers. In: *Proceeding of XXV A.T.I.V. international conference, Parma (Italy); 2010.* p. 34–8.
- [12] Froli M, Lani L. Adhesion, creep and relaxation properties of PVB in laminated safety glass. *Glass Int* 2011;34(7):33–8.
- [13] Van Duser A, Jagota A, Bennison SJ. Analysis of glass/polyvinyl butyral laminates subjected to uniform pressure. *J Eng Mech* 1999;125(4):435–42.
- [14] Behr RA, Minor JE, Linden MP. Load duration and interlayer thickness effects on laminated glass. *J Struct Eng* 1986;112(6):1441–53.
- [15] Hooper JA. On the bending of architectural laminated glass. *Int J Mech Sci* 1973;15:309–23.
- [16] Schuler C, Bucak Ö, Sackmann V, Gräf H, Albrecht G. Time and temperature dependent mechanical behaviour and durability of laminated safety glass. *Struct Eng Int* 2004;2:80–3.
- [17] Krüger G. Temperature effects on the structural behavior of laminated safety glass. *Otto Graf J* 1998;9:153–63.
- [18] Norville HS, King KW, Swofford JL. Behavior and strength of laminated glass. *J Eng Mech* 1998;124(1):46–53.
- [19] Ensslen F. Influence of weathering on the durability of laminated safety glass. In: *Proceedings of ISAAG 2006 conference, Munich; 2006.* p. 183–94.
- [20] Foraboschi P. Three-layered plate: elasticity solution. *Composites: Part B* 2014;60:764–76.
- [21] Foraboschi P. Hybrid laminated-glass plate: design and assessment. *Comp Struct* 2013;106:250–63.
- [22] Foraboschi P. Laminated glass column. *Struct Eng* 2009;87:20–6.
- [23] Foraboschi P. Behavior and failure strength of laminated glass beams. *J Eng Mech (ASCE)* 2007;133:1290–301.
- [24] Galuppi L, Royer-Carfagni G. Laminated beams with viscoelastic interlayer. *Int J Solids Struct* 2012;49:2367–645.
- [25] Sobek W, Kutterer M, Messmer R. Shear stiffness of the interlayer in laminated glass. In: *Proceedings of GPD1999 conference, Tampere (Finland); 1999.* p. 360–5.
- [26] Vallabhan CVG, Das YC, Ramasamudra M. Properties of PVB interlayer used in laminated glass. *J Mater Civ Eng* 1992;4(1):71–6.
- [27] Meissner M, Sackmann V. On the effect of artificial weathering on the shear bond and the tear strength of two different interlayers on laminated glass. In: *Proceedings of ISAAG 2006 conference, Munich; 2006.* p. 23–33.

- [28] Ferry JD. Viscoelastic properties of polymers. New York: Wiley; 1980.
- [29] Biolzi L, Castellani L, Pitacco I. On the mechanical response of short fibre reinforced polymer composites. *J Mater Sci* 1994;29(9):2507–12.
- [30] Dhaliwal AK, Hay JN. The characterization of polyvinyl butyral by thermal analysis. *Thermochim. Acta* 2002;391:245–55.
- [31] Roylance D. Mechanics of materials. New York: Wiley; 1996.
- [32] Gant FS, Bower MV. Domain of influence method: a new method for approximating Prony series coefficients and exponents for viscoelastic materials. *J Polym Eng* 1997;17(1):1–21.
- [33] Chan A, Liu XL, Chiu WK. Viscoelastic interlaminar shear modulus of fibre reinforced composites. *Compos Struct* 2006;75(1–4):185–91.